



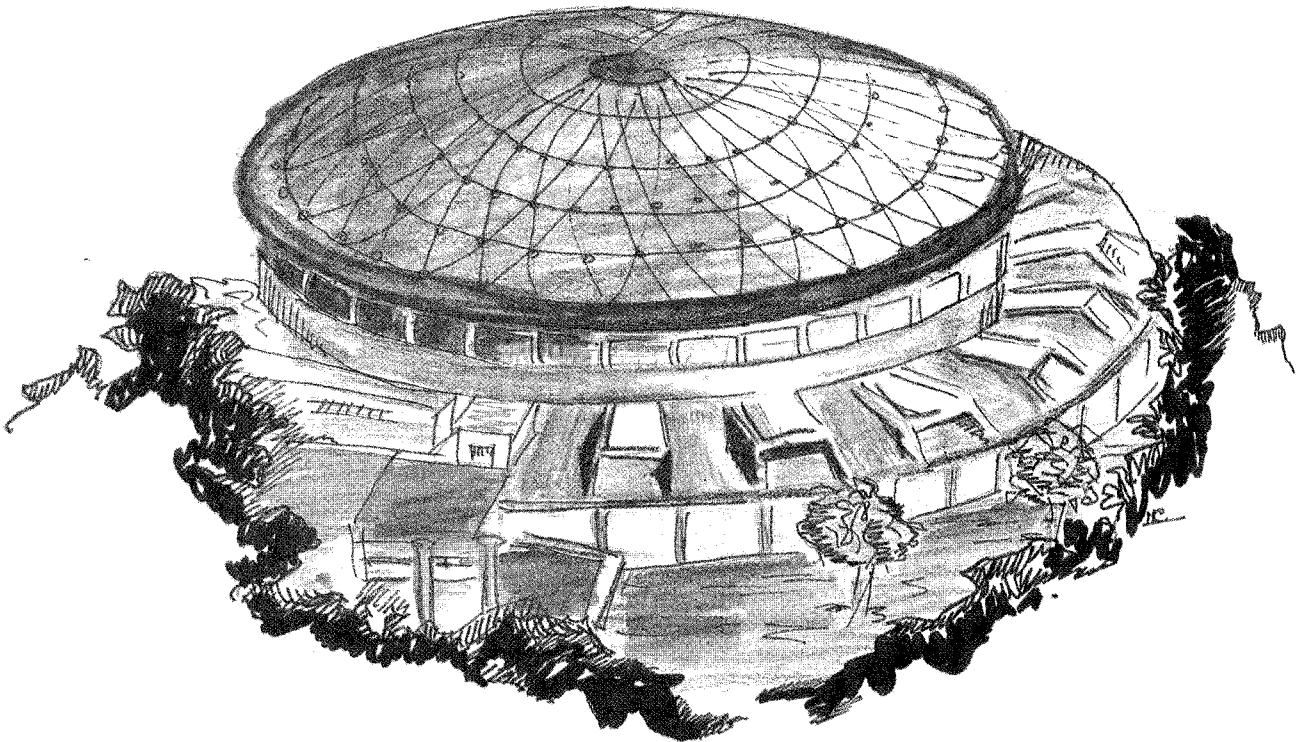
Laboratori Nazionali di Frascati

Submitted to Phys. Rev. C

LNF-88/50(P)
8 Settembre 1988

P. Levi Sandri, M. Anghinolfi, N. Bianchi, G.P. Capitani, P. Corvisiero, E. De Sanctis, C. Guaraldo, V. Lucherini, V. Muccifora, E. Polli, A.R. Reolon, G. Ricco, P. Rossi, M. Sanzone, M. Taiuti:

FORWARD AND BACKWARD ANGLES DIFFERENTIAL CROSS SECTION FOR DEUTERON PHOTODISINTEGRATION AT INTERMEDIATE ENERGIES



**FORWARD AND BACKWARD ANGLES DIFFERENTIAL CROSS
SECTION FOR DEUTERON PHOTODISINTEGRATION AT
INTERMEDIATE ENERGIES**

P. Levi Sandri*, M. Anghinolfi°, N. Bianchi*, G.P. Capitani*, P. Corvisiero°, E. De Sanctis*, C. Guaraldo*, V. Lucherini*, V. Muccifora*, E. Polli*, A.R. Reolon*, G. Ricco°, P. Rossi*, M. Sanzone, M. Taiuti.

* Istituto Nazionale di Fisica Nucleare - Laboratori Nazionali di Frascati,
I-00044 Frascati, Italy.

° Dipartimento di Fisica dell'Università di Genova and Istituto Nazionale di Fisica Nucleare-
Sezione di Genova, I-16146 Genova, Italy.

Abstract: The ${}^2\text{H}(\gamma, p)n$ cross section was measured simultaneously at $\vartheta_{p, \text{c.m.}} = 0^\circ, 90^\circ$ and 180° . The photon energy range was 98+243 MeV. A quasi-monochromatic photon beam was used and the photon spectrum measured on-line by a pair spectrometer. The results are in good agreement with the existing measurement of the 0° and of the 180° cross sections and confirm the consistency among all experimental data from monochromatic photon beams. At all measured energies, angular distributions were extracted and compared with theory. The agreement of theoretical calculations is highly improved with the introduction of terms of relativistic nature.

I. INTRODUCTION

Deuteron photodisintegration is the most extensively studied among all nuclear photoreactions, both from experimental and theoretical points of view. This is due to the fundamental role of this nucleus for our understanding of the nuclear properties: in fact, being a two body system, the deuteron wave function can be rigorously calculated if the forces are known; on the other hand, if the interaction is well established (as it is the case for the electromagnetic coupling), the comparison between theory and experiment is a clean test on the force involved between the two nucleons. From the experimental point of view, the

two body break-up of the deuteron offers important advantages with respect to other nuclear reactions since the measurement of the yield of protons emitted is directly related to the photodisintegration cross-section. Despite this simplicity, particular experimental care must be taken to obtain reliable absolute values of the cross-section; to this end, the use of quasi-monochromatic photon beams has led to a great improvement in the production of reliable experimental data sets¹.

An interesting particular case arises when the study of the differential cross section for deuteron photodisintegration is performed detecting protons emerging in the forward and backward directions. This is because at these angles the reaction is sensitive to the spin-dependent transition operators, the deuteron D state, non-central forces in the nucleon excited states and possible non-nucleonic phenomena.

Few years ago, Hughes *et al.*² have measured the 0° differential cross section of the deuteron photodisintegration over the photon energy range 20-120 MeV and found a disagreement with the standard Partovi³ calculation which, it was believed, should have been accurate within few percent if conventional ideas about two-nucleons interaction were at all correct. This result, later confirmed by measurements done in Louvain-la-Neuve^{4,5}, IUCF⁶ and Mainz⁷, initiated a number of attempts to reconcile theory with data, leading to the important observation made by Cambi Mosconi and Ricci,⁸ who, for the firsts, showed the importance of the relativistic correction to the impulse approximation cross-section.⁸⁺¹⁰

Apart from the mentioned experiments of Hughes *et al.*² and Zieger *et al.*,⁷ at 0°, and that of Althoff *et al.*,¹¹ at 180° and over the photon energy range 180-730 MeV, all previous angular distributions data of the deuteron photodisintegration process were taken at laboratory angles between ≈20° and ≈150°. Angular distributions were then assumed and extrapolations made to complete the plot of differential cross section versus center-of-mass angle at a fixed photon energy. The c.m. angular distribution expansion often assumed for this purpose was a sum of Légendre polynomials: $(d\sigma/d\Omega)_{c.m.} = \sum A_L(E_\gamma) P_L(\cos\vartheta_p^{c.m.})$, where $\vartheta_p^{c.m.}$ is the angle between the incoming photon and outgoing proton momenta in the center of mass and E_γ is the laboratory photon energy. This form is usually chosen because the orthogonality of the Légendre polynomials P_L ensures the relative independence of the fitted coefficients A_L .

In a previous paper¹², we compared the behaviors of the A_L coefficients obtained (up to $L=3$) by fitting data from monochromatic photon beams¹²⁺¹⁶ with those deduced by fitting the theoretical angular distribution calculations available at that time^{8,17,18}. The experimental total cross section $4\pi A_0$, as well as the interference coefficient A_1 were reasonably well reproduced by the theoretical predictions, while A_2 was strongly overestimated at energies greater than 100 MeV. The coefficient A_3 could not be determined as accurately as the other parameters: considering the error bars, its experimental values appeared in reasonable agreement with the calculation. However, especially above the pion photoproduction threshold, the conventional theory gives a different shape for the angular distributions (in

particular predicts too large values at forward and backward angles) compared to experiment. On this respect, one can remind that Shin *et al.*¹⁹, in order to investigate the dependence of the coefficients A_L , for $L \neq 0$, on the number of data points, found that the angular regions that principally affect the A_L values are those below 30° and above 140° in the lab. system.

From what said above, it is evident that a direct determination of the shape of the angular distribution at photon energy above 100 MeV, obtained with the simultaneous measurement of the differential cross section at $\vartheta_p^{c.m.} = 0^\circ, 90^\circ$ and 180° , can be very significant.

In this paper we present the results of a new measurement of the deuteron photodisintegration differential cross section at laboratory photon energies $E_\gamma = 98, 109, 118, 130, 143, 159, 174, 191, 211, 228,$ and 243 MeV, performed to get a deeper insight into the process by a combination of forward and backward cross section data in a new experimental approach. In fact, by detecting simultaneously the protons ejected at $\vartheta_p^{c.m.} = 0^\circ, 90^\circ$ and 180° , it is possible to determine the forward to backward ratio of the differential cross sections with reduced systematic errors and to check the absolute cross section value by means of the 90° detector. A preliminary account of this experiment, containing results with reduced statistics and relevant to only two photon energies, was recently published²⁰.

In section II the experimental procedure is described, followed by the data analysis method in section III; experimental results are contained in section IV together with the comparison with other recent experiments and with recent theoretical predictions; in section V we outline the consequences of this measurement with respect to different theoretical approaches while the conclusions are summarized in section VI.

II. EXPERIMENTAL PROCEDURE

The experiment was carried out at Frascati using the LEALE (Laboratorio Esperienze Acceleratore Lineare Elettroni) quasi-monochromatic photon beam produced by positron in flight annihilation on a liquid hydrogen target.²¹ In addition to monochromatic annihilation photons, bremsstrahlung is also produced: in order to increase the annihilation-to-bremsstrahlung photon ratio, measurements were carried out by collecting photons at an angle of 0.8° with respect to the positron direction. The total positron current intensity was measured in a Faraday cup while the cleaned and collimated photon beam was momentum analyzed by a pair spectrometer²² and its integrated flux was measured by a quantameter²³ that provides a constant sensitivity in our energy range. The simultaneous measurement of the photon beam total energy and spectrum allowed a 3% uncertainty in the determination of the annihilation peak intensity. The used photon flux was typically equal to about $5 \cdot 10^6$ annihilation photons per second. It is important to notice that the use of a quasi-monochromatic photon beam, though not strictly necessary for the measurement of a two-body reaction, offers important advantages making it possible to check unambiguously both

proton detector energy calibration and response function.

The layout of the experiment is schematically shown in Fig. 1. The deuterium target (whose density was continuously monitored and kept constant within 1%) consisted of a vertical mylar cylinder (40 mm diameter, 0.08 mm wall thickness), filled with liquid deuterium and inserted in the center of a dipole magnet which produced a uniform (within $\pm 0.5\%$) magnetic field inside a cylindrical volume, 20 cm high and 42 cm diameter. The protons were magnetically deflected out of the photon beam and detected by three dual-scintillator counter telescopes (called T0, T90 and T180), set at $\vartheta_p^{c.m.} = 0^\circ, 90^\circ$ and 180° respectively and connected on-line with a PDP 11/44 computer. The front counters (respectively 3 mm, 3 mm and 1 mm thick NE 102 scintillators) gave a measurement of the energy loss ΔE ; in order to ensure good homogeneity and optical efficiency, each front scintillator was coupled to two Philips 56 AVP type photomultipliers by means of a six sectors light guides²⁴. The back counters (10.4 cm diameter and 12 cm thick NaI crystals coupled to a Philips XP2041) gave a measurement of the kinetic energy E . The solid angles covered by the three telescopes were 1.8 msr (T0), 7.7 msr (T90) and 7.1 msr (T180). The gain stability of each photomultiplier was checked on-line every 10 minutes using two pulses generated by a green LED positioned on the edge of each scintillator, as described in ref. 25.

In order to correct for background protons from (γ, p) reactions in the target walls, windows, etc., measurements were performed with and without liquid deuterium in the target cell. The contribution under the peak of these background sources turned out to be $(12 \pm 18)\%$ for T0, $(2 \pm 5)\%$ for T90 and $(20 \pm 26)\%$ for T180, increasing with incident positron energy.

Details of the shielding differed markedly at the three angles where measurements were performed: at 90° shielding presented no serious problem whereas, in the forward and backward directions, where protons counters were necessarily set very close to the photon beam line, considerable additional shielding had to be introduced. Still, it was necessary to keep the beam path under vacuum in order to decrease the showering of photons in the air and to shield heavily the sides of this channel inside the magnet.

III. DATA ANALYSIS

Fig. 2 shows a typical photon energy spectrum measured on-line by the pair spectrometer at the given positron energy E_{e^+} , and collection angle of 0.8° ; the histogram represents the results of a Monte Carlo simulation code (PHOCHA²⁶) which also reproduces the measured ratio of the total photon beam energy over the total positron current intensity, respectively measured by the quantameter and by the Faraday cup. The excellent agreement between the computed and the measured spectra was obtained by slightly adjusting, by amounts within the experimental uncertainties, only the values of two input quantities, precisely positron beam emittance and photon collection angle.

Proton spectra were recorded at five positron energies, 120, 150, 180, 220 and 250 MeV, and simultaneously at the three angles. The measurements were made in four runs distributed over ten months and the data of each run were separately analyzed and compared. The results of different runs were found to be consistent within the statistical errors.

The stored data were presented on-line as a ΔE vs. E plot and the mass discrimination was found sufficiently good to distinguish unambiguously protons from other particles. Two different gain settings were used for the photomultipliers of the NaI crystals, one for the low energy runs (120 and 150 MeV) and one for the higher energies. Fig. 3 shows the ΔE vs. E plot of the events registered on-line from the three telescopes at the lowest and highest energy analyzed for each counter. As it can be seen, the mass discrimination between protons and other lighter particles (electrons and pions) is always good, especially in the high energy regions of the plot corresponding to photoprotons produced by annihilation photons. Because the rate of electromagnetic particles (electrons, positrons and subsequent showers) produced by the photon beam increases with the positron energy E_{e^+} and since this background is mainly forward directed, at $E_{e^+} = 250$ MeV the T0 telescope started suffering from pile-up effects that gave rise to an unbearable distortion of the proton energy spectrum; for this reason the 250 MeV run was not used to determine the 0° cross-section. On the other hand, before reaching the detector, protons undergo different degradation processes (nuclear absorption, straggling, multiple scattering, etc.); in the backward direction and at low energy those processes caused a too large distortion in the kinematical proton spectrum which could not be reliably taken into account; thus, the 120 MeV run was not used to determine the 180° cross-section.

As an example, the proton energy spectra (after subtraction of empty cell contribution) measured at $E_{e^+} = 180$ MeV are given in Fig. 4: as shown the peak due to the annihilation photon contribution is always clearly evident. The histograms represent the results of a Monte Carlo simulation code (D0180) used to account for the effects on the proton detectors due to finite photon beam size, extended target geometry and ray-tracing in the magnetic field. The program simulated the experimental photoproton spectra including for each event all the effects, such as solid angle, multiple scattering and energy losses in the target and scintillators, nuclear absorption and edge effects in the NaI crystals. Input data were the measured photon spectrum, the complete geometry of the apparatus, and a trial photodisintegration cross section which was iterated until the simulated spectra became compatible, within statistical errors, with the measured ones. The final iteration gave the experimental photodisintegration cross section with its uncertainty.

At first, only the peaks of the photon and proton spectra were used to obtain the cross section. Subsequently by means of the D0180 program it was possible to determine the cross section by using also part of the bremsstrahlung tail region, as already done in our previous paper.¹² Also in this measurement a good agreement was obtained among the values of the cross section (lab. system) extracted from the annihilation peaks and those deduced from the

bremsstrahlung tails. This allowed us to decrease the statistical error by means of a weighted average of the data. Because of this procedure, the relevant photon energies are slightly different from those published in our previous paper,²⁰ due to a different grouping of the NaI crystal channels.

IV. EXPERIMENTAL RESULTS

The center-of-mass values of the cross sections obtained from the five positron energy measurements were sorted into energy bins of slightly different wideness and combined to form one data set. The resulting cross section values as a function of the incoming photon energy for the three telescopes are listed in Table 1. The errors quoted are statistical only and do not include a $\pm 4.5\%$ systematic uncertainty (s.u.) obtained as the quadratic sum of the following contributions: uncertainty on the photon flux (3%), liquid deuterium target density (1%), solid angle from Monte Carlo (2%), energy calibration (2.5%).

The center-of-mass angular regions subtended by the three telescopes were $0.2^\circ + 2.6^\circ$ for T0 and $175.9^\circ + 180.7^\circ$ for T180 while for the T90 telescope the detected center-of-mass angle varied between $81.6^\circ + 86.6^\circ$ at $E_\gamma = 98$ MeV and $88.1^\circ + 93.1^\circ$ at $E_\gamma = 243$ MeV. In what follows these angular regions will be reported as $\vartheta_p^{c.m.} = 0^\circ, 90^\circ$ and 180° , for simplicity.

In Fig. 5 are shown the differential cross section values obtained from this experiment at the given photon energies. Also displayed in the figure are the recent data obtained with quasi-monochromatic photons from our previous work¹² (s.u. = $\pm 5\%$), with a bremsstrahlung beam and a Compton spectrometer by Hughes *et al.*² (s.u. = $\pm 3\%$), with bremsstrahlung photons by Althoff *et al.*¹¹ (s.u. = $\pm 6\%$), and with a tagged photon beam by Arends *et al.*¹⁵ (s.u. = $\pm 4\%$). In the same figure are also shown the data deduced by inverse reaction measurements by Meyer *et al.*⁶ (s.u. = $\pm 8\%$), and by Cameron *et al.*²⁷ (s.u. = $\pm 8\%$). As it results from the Figure, the new 90° values are always in good agreement within the total error with our previous data¹² although they are slightly lower at high energies. This result, obtained with a new experimental set-up, shows the reproducibility of our earlier data and confirms the reliability of the deuteron photodisintegration differential cross section values measured by using monochromatic photon beams. Also recent preliminary results obtained at Mainz²⁸ in a tagged photon experiment at $130 + 150$ MeV (not shown in the figure) are in good agreement with our values.

The consistency among results from monochromatic photon measurements is most clearly seen if values of the total cross section are plotted as a function of the photon energy as shown in Fig.6 and listed in Table 2. Our data points ($\sigma_T = 4\pi A_0$) were obtained fitting to a sum of Légendre polynomials the combined angular distributions obtained from this measurement and from our previous work.¹² The other values are the data measured at low energy by Bernabei *et al.*¹⁴, those given at high energy by Arends *et al.*¹⁵ and those we deduced by fitting the angular distributions from radiative capture measurements^{6,27,29}. In all

cases the quoted systematic error in the experiment was linearly added to the statistical one. As we can see, a good agreement is obtained for the total cross-section values showing again that the use of monochromatic photons beams highly increases the quality of the data, particularly in the Δ -resonance region where the use of bremsstrahlung photon beams caused discrepancies among different experiments by a factor of two.¹ Therefore values obtained with monochromatic measurements represent a reasonable basis of experimental data to compare with theoretical calculations.

V. DISCUSSION

In Fig.7 the experimental angular distributions of Fig.5 are compared with the available recent theoretical results and specifically with the calculation performed by Cambi, Mosconi and Ricci (CMR)⁸, Jaus and Woolcock (JW)¹⁰, Laget¹⁷, Wilhelm, Leidemann and Arenhövel (WLA)³⁰, and Rustgi, Vyas and Rustgi (RVR)³¹. CMR, JW and RVR have studied the process below the pion photoproduction threshold including meson exchange effects and relativistic corrections to the one-body and two-body charge density operators. The diagrammatic approach of Laget and the coupled channel calculation of WLA, which contain also isobar configurations, can be extended up to the Δ -resonance region. Both these calculations include only partial relativistic effects and final state interactions.

At $E_\gamma = 100$ MeV the angular distribution is well reproduced by all recent theoretical approaches, as it is shown in Fig.7, where the shadowed region indicates the area spanned by different calculations^{8+10,17,30,31}. As the energy increases the agreement becomes less satisfactory. At $E_\gamma = 145$ MeV the theory predicts a more isotropic angular distribution than observed, in particular around $\vartheta_p^{c.m.} = 90^\circ$ the theoretical cross-section values are $\approx 20+30\%$ lower than the experimental ones. Above the pion photoproduction threshold, a fewer number of calculations are available. For those energies, in Fig.7 are given the recent theoretical results of Laget¹⁷ and of WLA³⁰ performed at $E_\gamma = 175$ and 210 MeV: the shape of the angular distributions is substantially well predicted by the two approaches but, in the central angular region, both calculations still underestimate the experimental cross section.

A further comparison between theory and experiment can be performed by investigating the excitation functions measured at fixed angle vs. incoming photon energy, as displayed in Fig.8. The upper part of the figure shows our results for the 0° differential cross-section together with the existing values obtained by Hughes *et al.*² and by Zieger *et al.*⁷; also shown in the figure are the values deduced by inverse reaction measurement by Ninane *et al.*⁴, Dupont *et al.*⁵, and Meyer *et al.*⁶. The lower part of the figure shows the 180° differential cross-section obtained from this measurement together with the data from Althoff *et al.*¹¹ and with the low energy point from radiative capture measurement of Ninane *et al.*⁴. As one can see from the figure there is a remarkable agreement among the existing data both at 0° and at 180° . Also shown in the figure are the results from CMR, from Laget and from

WLA. (other calculations performed below the pion threshold^(9,10,31) give results similar to CMR and are hereafter omitted for simplicity). All different theoretical approaches give a quite similar behavior for the excitation functions but differ among each other in the absolute value of the cross section. As it results from the figure, all the performed calculations show some discrepancies with respect to the experimental values; the Laget approach reproduces better the experimental data points of the 0° excitation function except at high energies (above 140 MeV), where it underestimates the data by a factor of about 20%. However, it must be noticed that especially in the Δ region, calculations are still model dependent and different potentials give different absolute values while keeping the overall behavior of the cross section.

An important feature of this experiment is that the simultaneous measurement at the three most important and critical angles allows to determine ratios between these values with reduced systematic uncertainties and in particular free from the uncertainties arising from the photon flux and target density that, for most of the experiments, represent the major part of the systematic error. The ratios deduced from this measurement are shown in Fig.9 together with the value obtained at low energy by a neutron capture experiment⁴ and with the extrapolated values from De Pascale *et al.*¹³ Also shown in the figure are some of the theoretical predictions^{8,17,30}. As one can see, R1 ($\equiv d\sigma(0^\circ)/d\sigma(180^\circ)$) is predicted by all theories to be substantially constant in the range 100+210 MeV and with value around 1.25. The experimental value of this ratio increases slightly with energy, but the discrepancy with theory is not large. A different situation is found examining the R2 ($\equiv d\sigma(0^\circ)/d\sigma(90^\circ)$) and the R3 ($\equiv d\sigma(180^\circ)/d\sigma(90^\circ)$) ratios of cross-sections: in fact, while at low energy the calculations fit nicely the data points, above 100 MeV they clearly overestimate the experimental results showing once more that, in this energy region, the angular distributions are less isotropic than predicted by theory.

CONCLUSIONS

The cross-section for deuteron photodisintegration was simultaneously measured at 0° , 90° and 180° at intermediate energy using quasi-monochromatic photons. The new cross section values agree with our previous results and with the other monochromatic data available in the literature. These data provide a reliable set that was compared to theoretical calculations. It is found that, below the pion production threshold, the current theory reproduces well the experimental results. In the Δ region, the predicted angular distributions are too isotropic with respect to the experimental ones. It is also shown that the inclusion of terms of relativistic origin in the theories is necessary to reproduce the general behavior of angular distributions. Since the theoretical approaches contain different approximations, a complete and systematic study of the photodisintegration of deuteron is highly needed to check whether this process can be described in the classic framework of nuclear physics (that

is, considering only nucleonic and mesonic degrees of freedom) or if new degrees of freedom have to be included in the picture of the reaction mechanism.

We acknowledge the LEALE and Genova technical staffs for their assistance during the experiment and the linac crew for running efficiently the accelerator.

References

1. M.Sanzone, Proceedings of the International School of Intermediate Energy Nuclear Physics, Verona 20+30 June 1985, p. 78. R. Bergère, S Costa and C. Schaerf editors. World Scientific 1986.
2. R.J. Hughes, A. Zieger, H. Wäffler and B. Ziegler, Nucl. Phys. **A267**, 329 (1976).
3. F. Partovi, Ann. of Phys. **27**, 79 (1964).
4. A. Ninane, C. Dupont, P. Leleux, P. Lipnik and P. Macq, Can.J.Phys. **62**, 1104 (1984).
5. C.Dupont, P. Leleux, P. Lipnik, P. Macq and A. Ninane, Nucl. Phys. **A445**, 13 (1985).
6. H.O. Meyer, J.R. Hall, M. Hugi, H.J. Karwowsky, R.E. Pollock and P. Schwandt, Phys. Rev. **C31**, 309 (1985).
7. A. Zieger, P. Grewer and B. Ziegler, Few-Body Systems **1**, 135 (1986).
8. A. Cambi, B. Mosconi and P. Ricci, Phys. Rev. **C26**, 2358, (1982) and J. Phys. **G10**, L11 (1984).
9. J.L.Friar, B.F. Gibson and G.L. Payne, Phys. Rev. **C30**, 441 (1984); and J.L.Friar, private communication.
10. W.Jaus and W.S. Woolcook, Nucl. Phys. **A431**, 669, (1984); and **A473**, 667 (1987); and **A473**, 685 (1987).
11. K.H. Althoff, G. Anton, D. Bour, B. Bock, W. Ferber, H.W. Gelhausen, N. Horikawa, Th. Jahnen, O. Kaul, W. König, K.C. Königsmann, D. Menze, W. Meyer, Th. Miczaika, E. Roderburg, W. Ruhm, E.P. Shilling, W. Schwille, D. Sundermann and K.Wagener, Z. Phys. **C21**,149 (1983).
12. E. De Sanctis, M. Anghinolfi, G.P. Capitani, P. Corvisiero, P. Di Giacomo, C. Guaraldo, V. Lucherini, E. Polli, A.R. Reolon, G. Ricco, M. Sanzone and A. Zucchiatti, Phys. Rev. **C34**, 413 (1986).
13. M.P. De Pascale, G. Giordano, G. Matone, D. Babusci, R. Bernabei, O.M. Bilianuk, L. Casano, S. d'Angelo, M. Mattioli, P. Picozza, D. Prospero and C. Schaerf, Phys. Rev. **C32**, 1830 (1985).
14. R. Bernabei, A. Incicchitti, M. Mattioli, P. Picozza, D. Prospero, L. Casano, S. d'Angelo, M.P. De Pascale, C. Schaerf, G. Giordano, G. Matone, S. Frullani and B. Girolami, Phys. Rev. Lett. **57**,1542 (1986).
15. J. Arends, H.J. Gassen, A. Hegerath, B. Mecking, G. Nöldeke, P. Prenzel, T. Reichelt, A. Voswinkel and W.W. Sapp, Nucl. Phys. **A412**, 509 (1984).
16. K. Baba, I. Endo, H. Fukuma, K. Inoue, T. Kawamoto, T. Ohsugi, Y. Sumi, T. Takeshita, S. Uehara, Y. Yano and T. Maki, Phys. Rev. **C28**, 286 (1983).
17. J.M. Laget, Nucl. Phys. **A312**, 265, (1978); and Can.J. Phys. **62**, 1046 (1984); and private communication.
18. W.Leidemann and H.Arenhövel, Phys.Lett.**139B**, 22 (1984); and Can.J.Phys. **62**,1036 (1984).
19. Y.M. Shin, J.A. Rawlins, W. Buss and A.O. Evwaraye, Nucl. Phys. **A154**, 482 (1970).
20. P. Levi Sandri, E. De Sanctis, M. Anghinolfi, N. Bianchi, G.P. Capitani, P. Corvisiero, C. Guaraldo, V. Lucherini, V. Muccifora, E. Polli, A.R. Reolon, G. Ricco, P. Rossi, M. Sanzone and M. Taiuti, Phys. Rev. Lett. **59**, 2543 (1987).
21. G.P. Capitani, E. De Sanctis, P. Di Giacomo, C. Guaraldo, V. Lucherini, E. Polli, A.R. Reolon, R. Scrimaglio, M. Anghinolfi, P. Corvisiero, G. Ricco, M. Sanzone and A. Zucchiatti, Nucl. Instr. and Meth. **216**, 307 (1983).
22. G.P. Capitani, E. De Sanctis, P. Di Giacomo, C. Guaraldo, V. Lucherini, E. Polli, A.R. Reolon and R. Scrimaglio, Nucl. Instr. and Meth. **178**, 61 (1980).
23. A. P. Komar, S.P. Kroglov and I.V. Lopatin, Nucl. Instr. and Meth. **82**, 125 (1970).
24. A. Zucchiatti, M. Sanzone and E. Durante, Nucl. Instr. and Meth. **129**, 467 (1975).

25. M. Anghinolfi, M. Castoldi, M. Albicocco and E. Polli, *Nuovo Cimento* **88A**, 257 (1985).
26. E. De Sanctis, V. Lucherini and V. Bellini, *Comp. Phys. Comm.* **30**, 71 (1983).
27. J.M. Cameron, C.A. Davis, H. Fielding, P. Kitching, J. Pasos, J. Soukup, J. Uegaki, J. Weisick, H.S. Wilson, R. Abegg, D.A. Hutcheon, C.A. Miller, A.W. Stetz and I.J. Van Heerden, *Nucl. Phys.* **A458**, 637 (1986).
28. J. Annand, P. Wallace, G. Crawford, S. Hall, J. Kellie, J.C. Mc George, D. Macgregor, R.O. Owens, R. Beck, D. Yrmscher, H. Schmieder, B. Schoch and J. Vogt, *Physics with MAMI A*, Mainz, May 1988; and R.O. Owens, private communication.
29. M. Hugi, J.M. Cameron, M. Ahmad, J. Collot, G. Gaillard, J. Weisick, G.W.R. Edwards, H. Fielding, D.A. Hutcheon, R. Abegg, C.A. Miller, P. Kitching, N.E. Davison, N.R. Stevenson and I.J. Van Heerden, *Nucl. Phys.* **A472**, 701 (1987).
30. P. Wilhelm, W. Leidemann and H. Arenhövel, *Few-Body Systems* **3**, 111 (1988); and private communication.
31. M.L. Rustgi, R. Vyas and O.P. Rustgi, *Phys. Rev.* **C29**, 785 (1984).

figure captions

Fig.1. Schematic view of the experimental apparatus used in this measurement.

Fig. 2. Photon spectrum recorded by the pair spectrometer at $E_{e^+} = 180$ MeV and at a photon collection angle of 0.8° . The histogram is the result of the Monte Carlo code PHOCHA.

Fig. 3. ΔE vs. E plot of events for the three telescopes at the lowest and highest analyzed energies.

Fig. 4. Proton spectra as recorded at incoming positron energy $E_{e^+} = 180$ MeV by the three telescopes after subtraction of empty cell contribution. The histogram shows the results of Monte Carlo code D0180.

Fig. 5. Some of the angular distributions obtained in this experiment at the given photon energies; full circles: this work; empty diamonds: ref. 2; empty triangles: ref. 6; crosses: ref. 11; empty circles: ref. 12; empty squares: ref. 15; full triangles: ref. 27. Only statistical error is included; where not visible, error is within the spot of the experimental point.

Fig. 6. Total cross section values obtained from the fitting procedure described in the text. Full circles: this work and ref. 12; down triangles: ref. 6; full squares: ref. 14; empty squares: ref. 15; up triangles ref. 27 and 29.

Fig. 7. Comparison of experimental and theoretical angular distributions. Notation as in Fig. 6. Shaded area is spanned by calculations of ref. 8,9,10, 17, 30 and 31. Dotted line: ref. 17, full line: ref. 30; .

Fig. 8. Excitation functions vs. incoming photon energy at $\vartheta_p = 0^\circ$ and 180° . Full circles: this work; empty diamonds: ref. 2; down triangles: ref. 4 and 5; up triangles: ref. 6; full diamonds: ref. 7; crosses: ref. 11. dashed line: ref. 8; dotted line: ref. 17; full line: ref. 30.

Fig. 9. Ratio of cross sections obtained from this experiment (full circles) together with the data point of ref. 4 (triangle) and with the extrapolated values of ref. 13 (full squares) compared to theoretical calculations including relativistic corrections. For the curves, notation as in Fig. 8.

Table 1. Values (in $\mu\text{b}/\text{sr}$) of the center-of-mass differential cross-section for deuteron photodisintegration at the three nominal measured angles. The errors quoted are statistical only and do not include a $\pm 4.5\%$ systematic uncertainty.

E_γ (MeV)	$\vartheta_p^{\text{c.m.}} = 0^\circ$	$\vartheta_p^{\text{c.m.}} = 90^\circ$	$\vartheta_p^{\text{c.m.}} = 180^\circ$
95 + 105	4.06 \pm 0.44	6.84 \pm 0.23	-----
104 + 114	3.84 \pm 0.43	6.59 \pm 0.18	-----
114 + 122	3.93 \pm 0.32	6.26 \pm 0.15	-----
124 + 136	3.63 \pm 0.27	5.36 \pm 0.17	2.59 \pm 0.16
136 + 150	3.53 \pm 0.23	5.02 \pm 0.14	2.35 \pm 0.13
151 + 167	4.00 \pm 0.30	4.59 \pm 0.18	2.44 \pm 0.16
167 + 184	3.96 \pm 0.26	4.87 \pm 0.20	2.44 \pm 0.17
182 + 200	4.63 \pm 0.47	5.29 \pm 0.24	2.48 \pm 0.33
202 + 220	4.87 \pm 0.28	5.39 \pm 0.19	2.92 \pm 0.23
220 + 236	-----	5.08 \pm 0.55	3.15 \pm 0.39
236 + 250	-----	5.59 \pm 0.40	3.66 \pm 0.37

Table 2. Values of the total cross-section ($4\pi A_0$); errors include both the statistical and the systematic uncertainty linearly added.

E_γ (MeV)	$4\pi A_0$ (μb)	ref.
14.7	925.0 \pm 64.0	14
19.3	617.0 \pm 40.0	"
28.9	361.0 \pm 18.0	"
38.2	249.0 \pm 12.0	"
47.5	177.0 \pm 9.0	"
57.5	139.0 \pm 8.0	"
74.	97.6 \pm 8.3	"
95.	72.6 \pm 11.5	6
98.	69.7 \pm 4.0	12 + this work
100.	70.9 \pm 4.3	27
109.	66.7 \pm 3.8	12 + this work
118.	63.1 \pm 3.8	"
130.	55.8 \pm 4.4	"
140.	52.8 \pm 2.7	27
143.	53.7 \pm 3.3	12 + this work
159.	53.5 \pm 3.3	"
174.	56.2 \pm 3.4	"
187.	49.1 \pm 7.6	29
191.	60.1 \pm 4.1	12 + this work
200.	53.7 \pm 2.8	15
211.	65.6 \pm 4.2	12 + this work
220.	58.3 \pm 2.9	15
228.	67.9 \pm 5.2	12 + this work
240.	62.7 \pm 3.0	15
243.	68.9 \pm 4.9	12 + this work
260.	65.2 \pm 3.2	15
280.	65.0 \pm 3.2	"
300.	60.2 \pm 3.0	"
320.	52.2 \pm 2.7	"
340.	45.3 \pm 2.3	"
360.	34.3 \pm 1.8	"
380.	26.0 \pm 1.4	"
400.	20.2 \pm 1.3	"
420.	16.1 \pm 1.0	"
440.	11.9 \pm 1.0	"

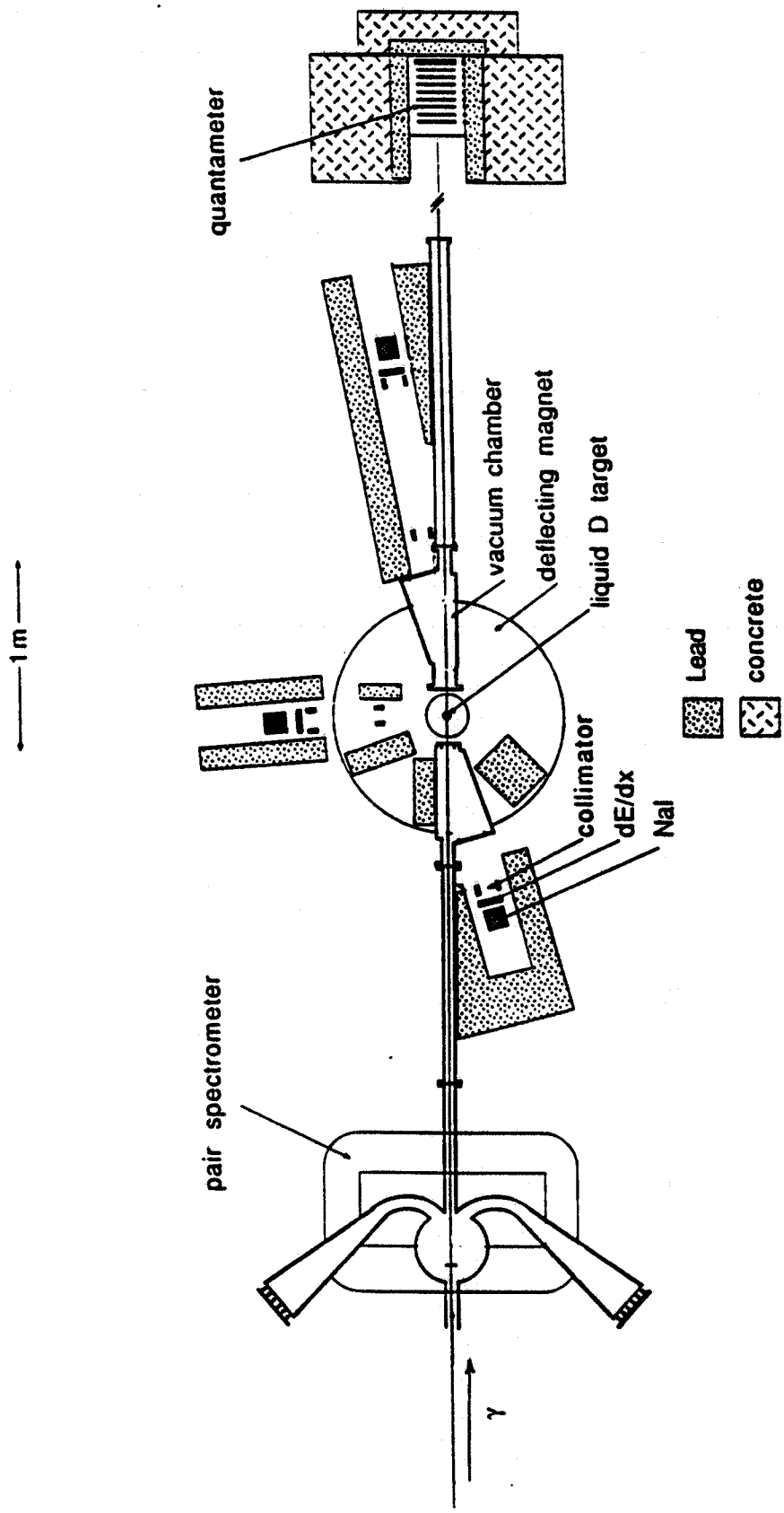


Fig. 1

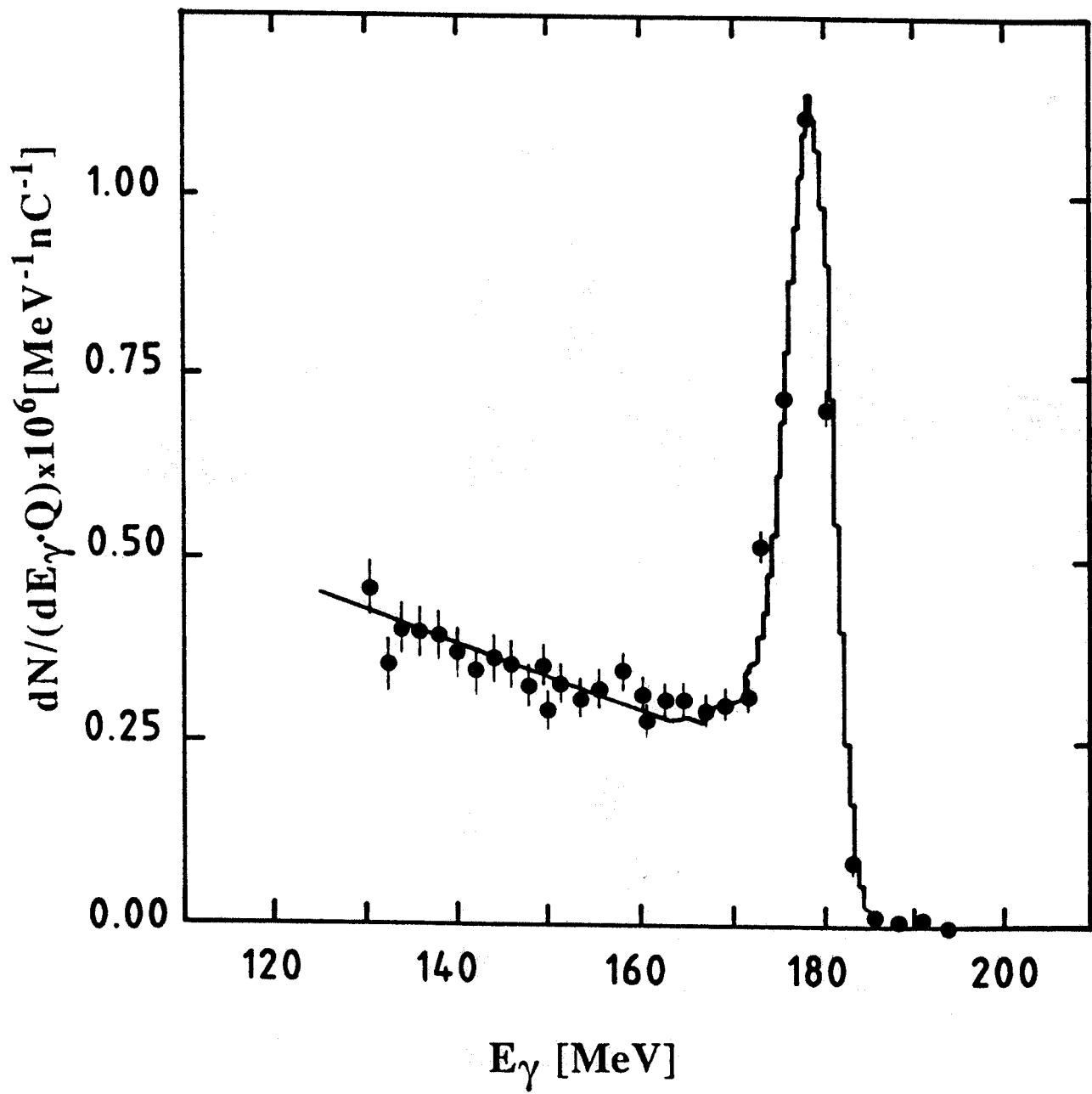
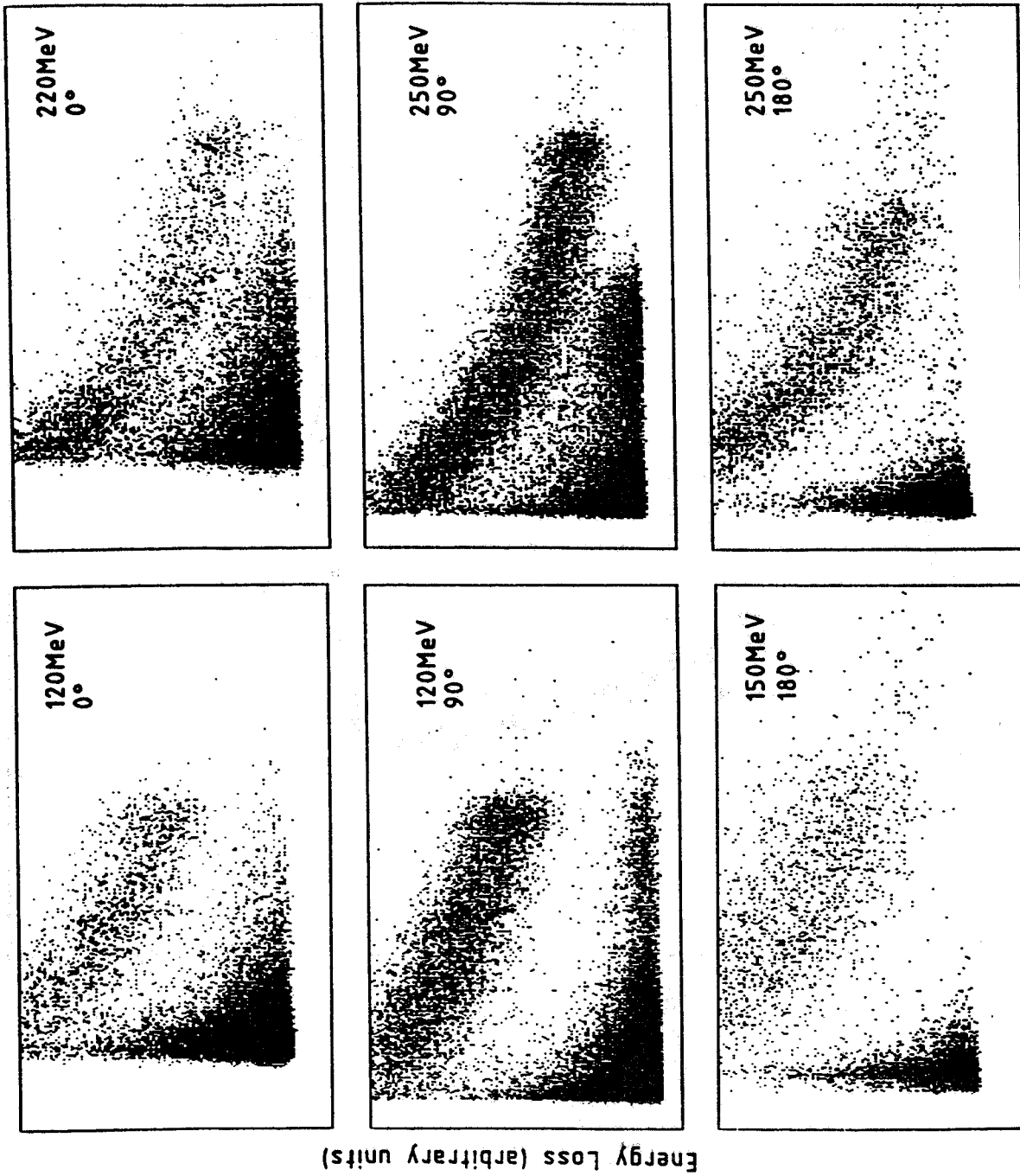


Fig. 2



Energy (arbitrary units)

Fig. 3

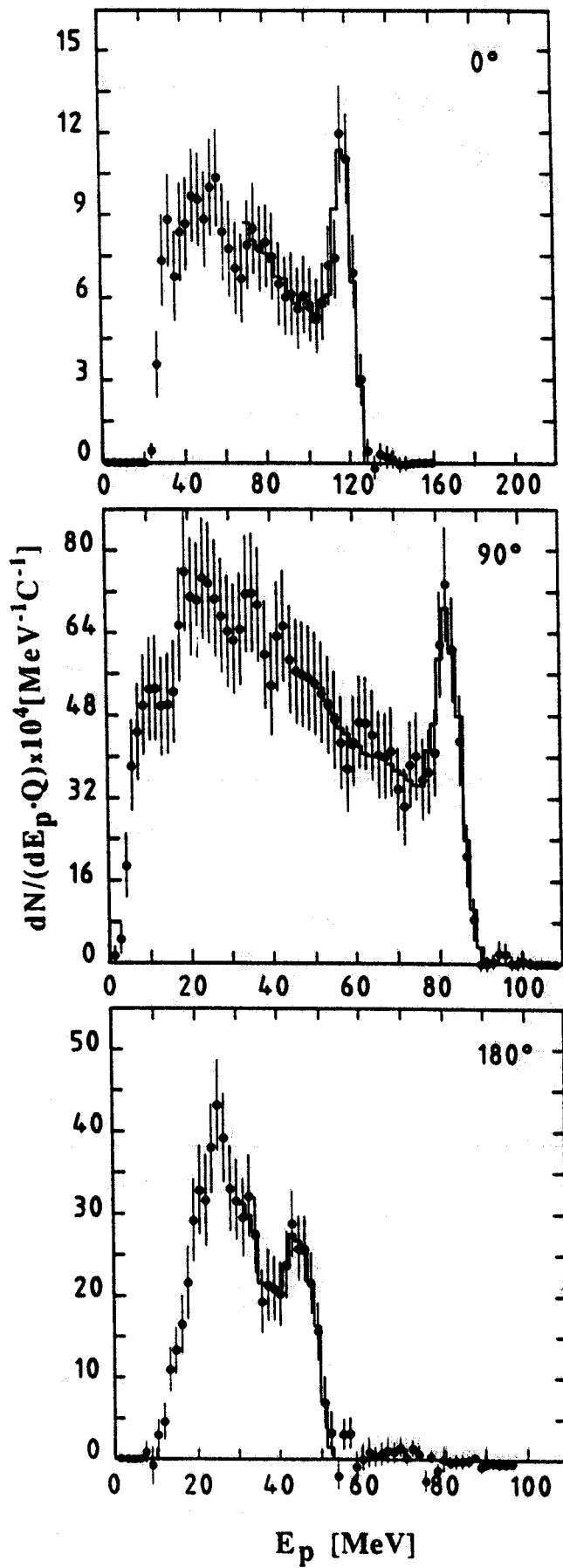


Fig. 4

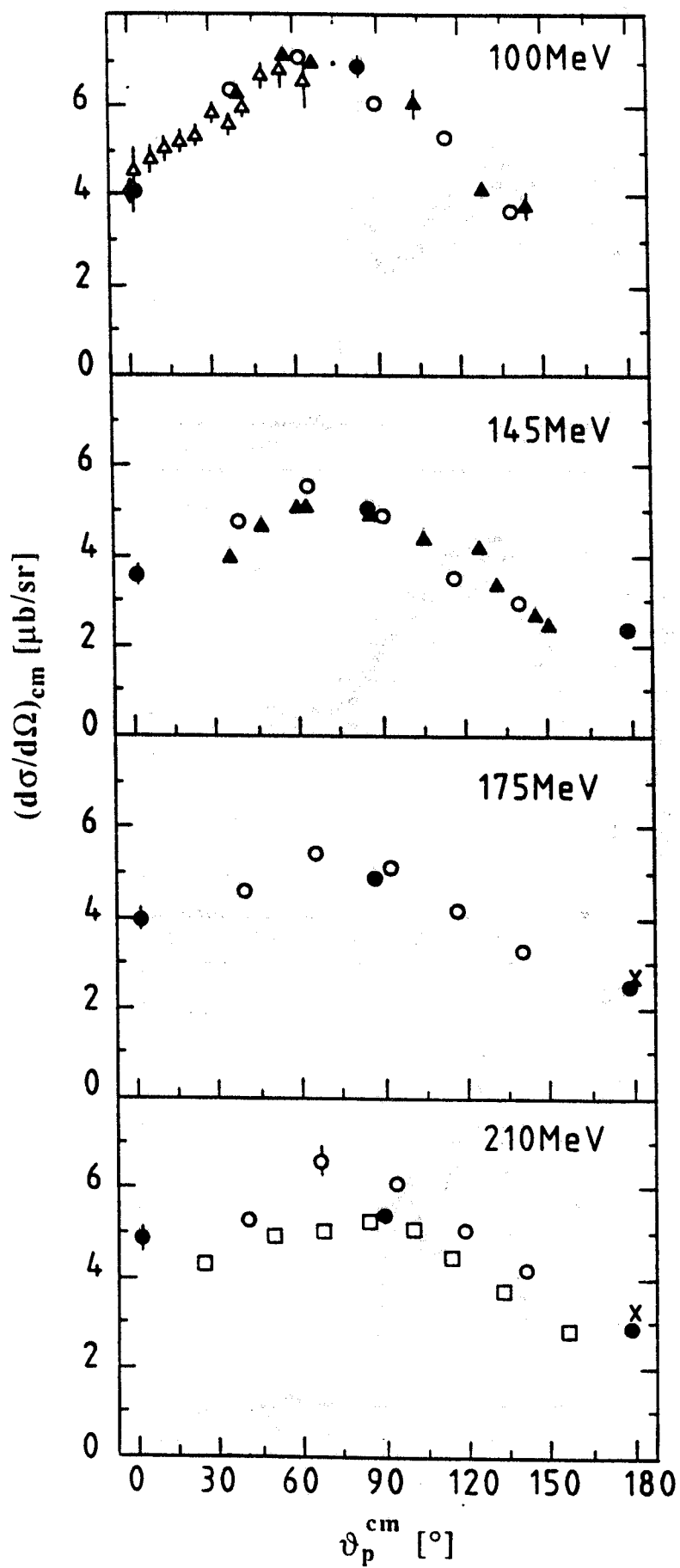


Fig. 5

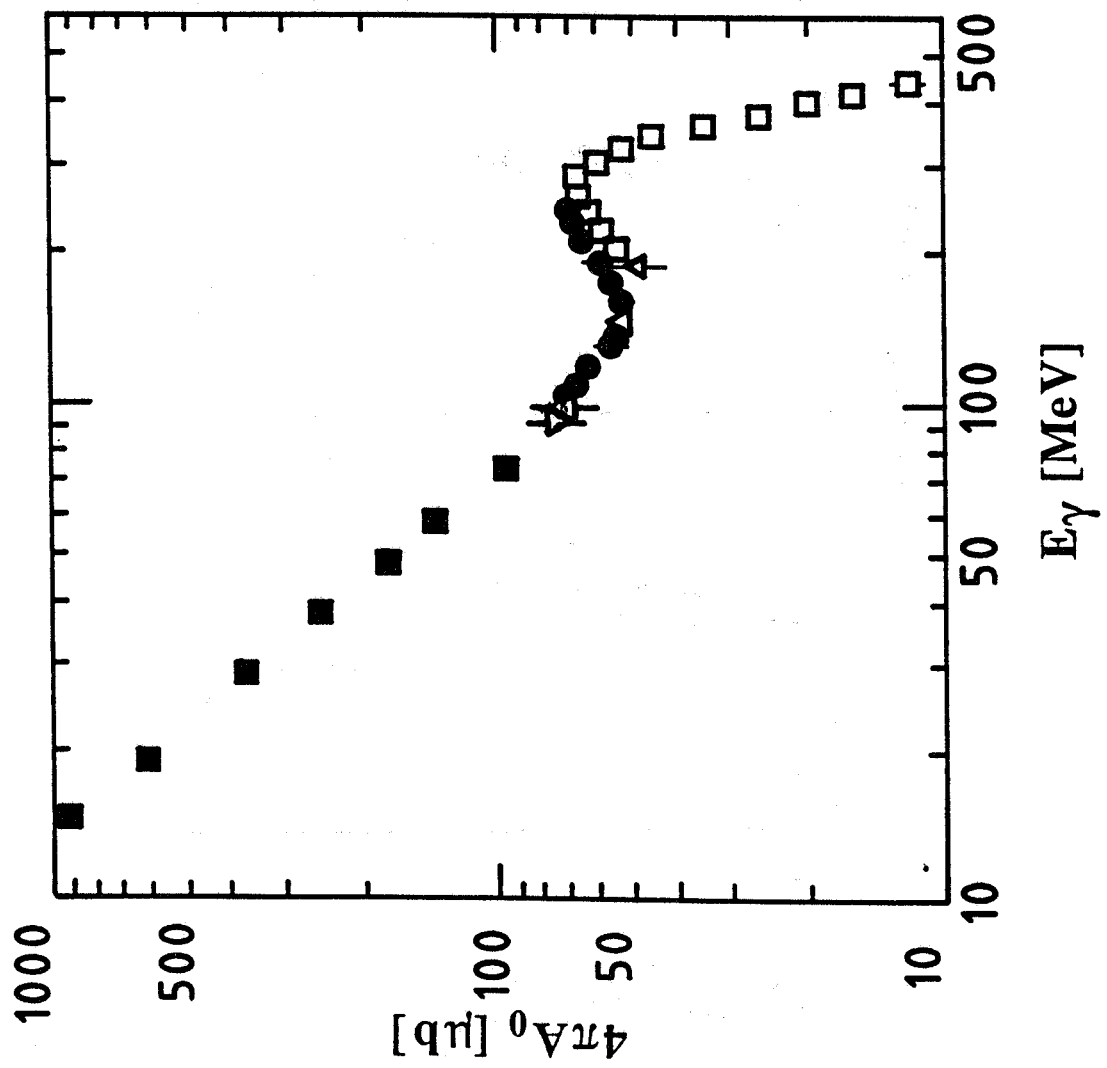


Fig. 6

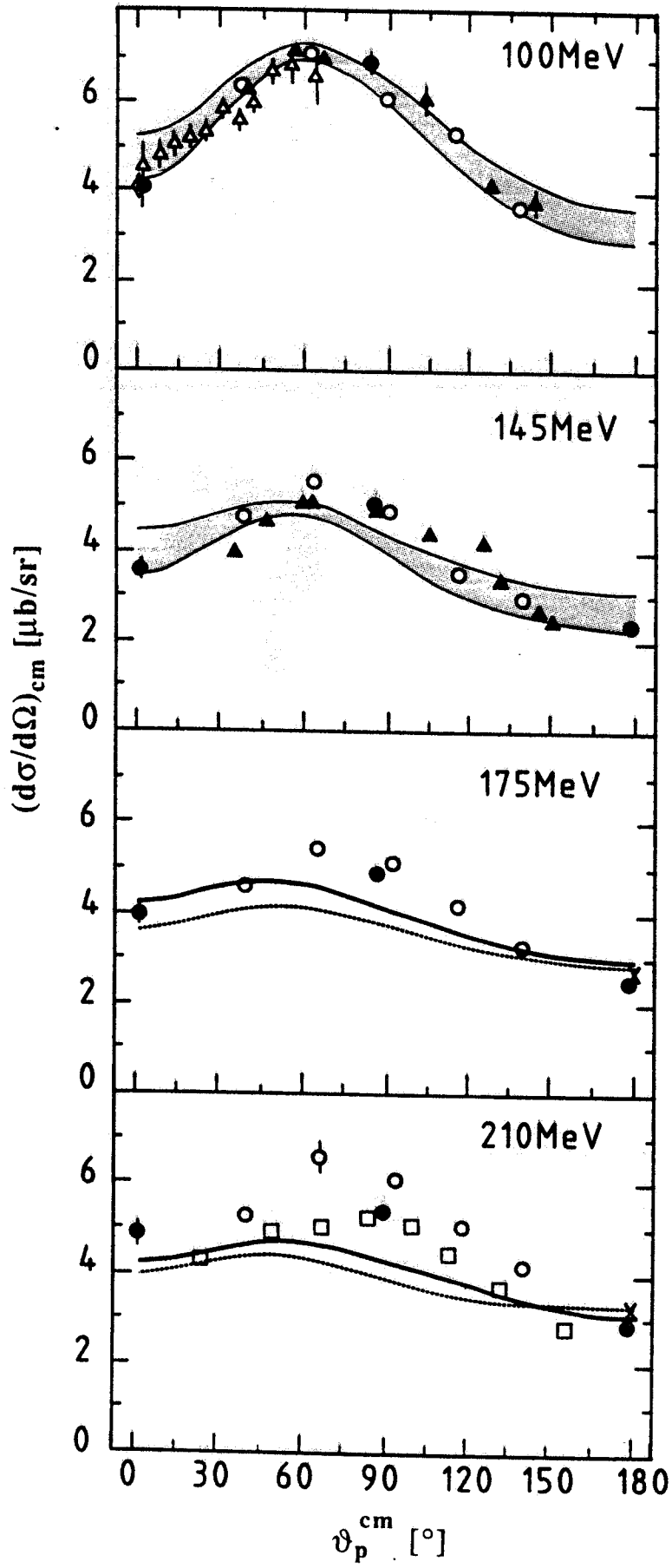


Fig. 7

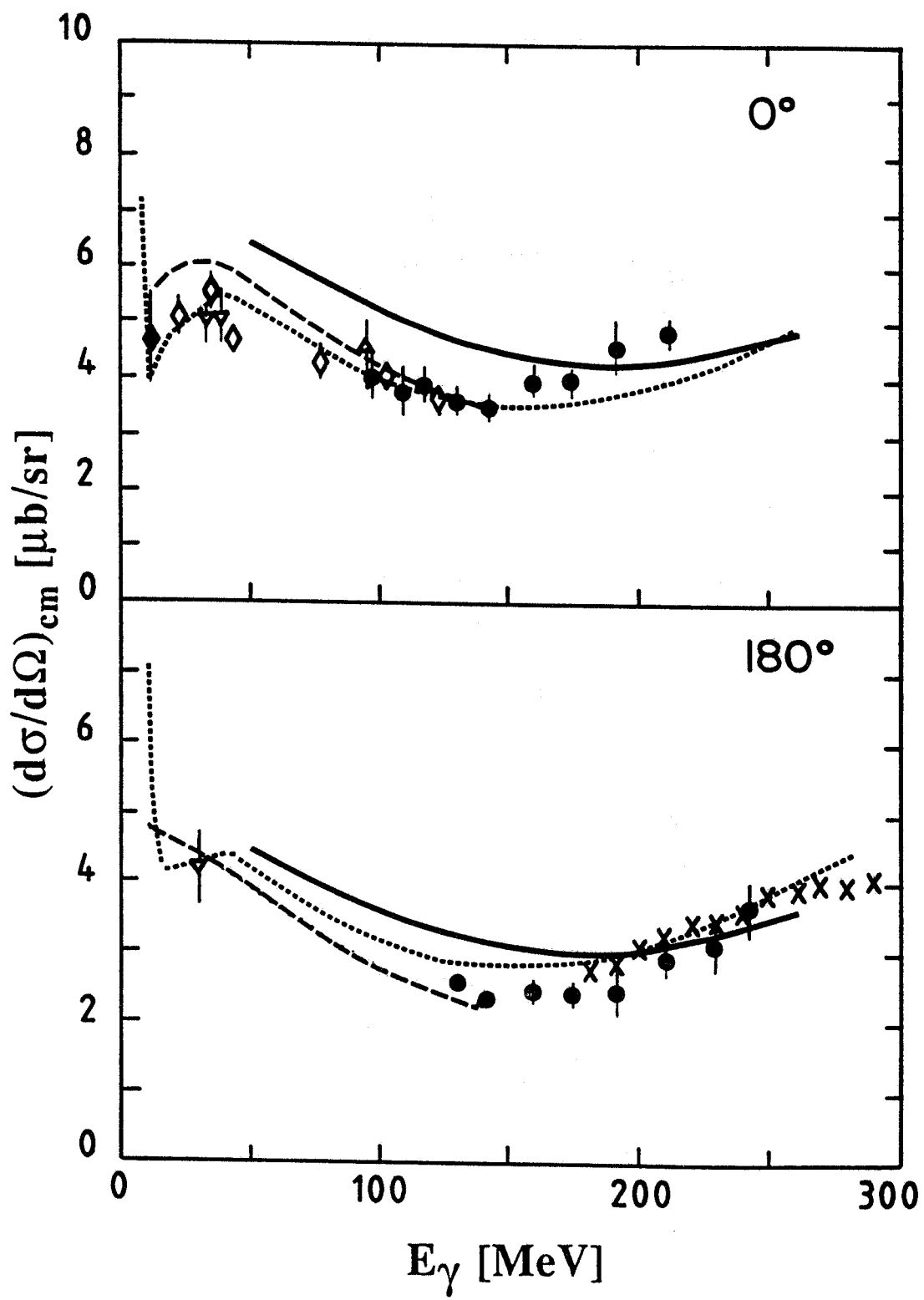


Fig. 8

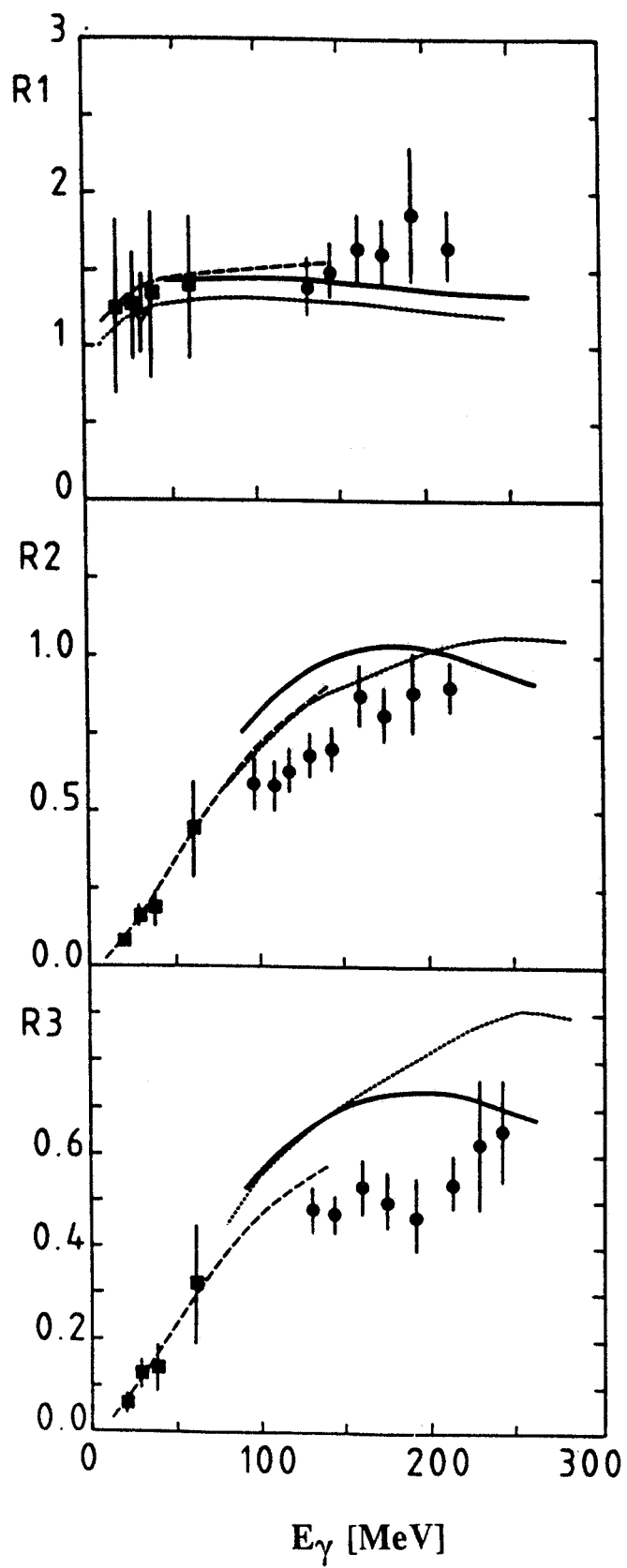


Fig. 9